Atomic inner-shell x-ray laser pumped by an x-ray free-electron laser

Nina Rohringer and Richard London
Lawrence Livermore National Laboratory, Livermore, California 94551, USA
(Received 25 February 2009; revised manuscript received 8 June 2009; published 14 July 2009)

We discuss possibilities of pumping an atomic inner-shell x-ray laser with an x-ray free-electron laser (XFEL). Self-consistent gain calculations show that with the first available XFEL, the Linac Coherent Light Source at Stanford, it will become possible to produce subfemtosecond x-ray pulses at intensities reaching 6×10^{16} W/cm^2. Small-signal gain calculations indicate that saturation of more than one lasing line is possible, resulting in temporally separated femtosecond x-ray pulses of different wavelengths. The presented lasing scheme creates broad capability for advancing the field of high-intensity ultrashort x-ray physics.

DOI: 10.1103/PhysRevA.80.013809 PACS number(s): 42.55.Vc, 32.80.Aa, 41.60.Cr, 42.65.Re

Laboratory atomic x-ray lasers (XRLs) were first realized in 1984 [1]. Since then, a world-wide community has worked to advance the parameters and application of these sources. The shortest wavelength achieved so far is 3.6 nm, albeit with a weak output [2]. More recently, x-ray free-electron lasers (XFELs) have been proposed [3] and there are currently three XFEL facilities under construction. We propose to merge these two technologies by pumping an atomic XRL with a radiation pulse from an XFEL. Saturated XRL pulses with peak intensities comparable to XFELs and wavelengths of 1.5 nm or less can be achieved. A variety of different pulse shapes are possible: transform limited, single x-ray pulses of subfemtosecond duration, x-ray pulses in the range of 10 fs duration with improved coherence properties, and a series of temporally separated femtosecond x-ray pulses of different wavelengths. This can build the basis for two-color pump-probe experiments in the x-ray regime.

Forthcoming XFEL sources will be based on the self-amplified spontaneous emission (SASE) process [4], creating quasichaotic pulses, containing uncorrelated intensity spikes of femtosecond duration [5]. Our proposed scheme holds the potential of isolating single femtosecond spikes and creating radiation of increased temporal coherence, thereby smoothing the chaotic pulse profile of SASE radiation. Several communities could benefit from this new ultrafast x-ray source. The time resolution for techniques such as x-ray photoelectron spectroscopy [6] and x-ray diffraction of solids [7] could be improved. Pump-probe techniques such as femtosecond transient absorption spectroscopy [8] could be transferred to the x-ray regime. Controlling the pulse duration, it would become possible to study x-ray nonlinear quantum optical effects in the time domain [9,10].

The quest for ultrashort high-intensity x-ray sources is being tackled with several techniques. Proposals to produce femtosecond x-ray pulses at XFEL facilities are based on slicing of the electron beam [11] or operation with low-charge ultralow emittance electron beams [12]. Lately, a scheme to produce a train of attosecond pulses by mode locking of an XFEL was proposed [13]. At the other end of the spectrum are optical laser pumped XRLs seeded with high-harmonic radiation [14]. Due to the lack of high-harmonic radiation at shorter wavelength, this method is currently limited to the soft x-ray regime (>10 nm). Recently, the idea of using an FEL to pump a laser in the xuv regime was put forward for an inner-shell lasing scheme of carbon [15] and a recombination-based soft XRL of helium [16]. Another approach aims for pumping an XRL with broadband betatron radiation [17]. We propose a lasing scheme of broad capability by photopumping an inner-shell XRL [18] with an XFEL. The method can be applied to a broad variety of gain materials. In this paper we present gain calculations for neon, tailored to predict first lasing experiments using the Linac Coherent Light Source (LCLS) at Stanford.

Focusing the XFEL into a gas target, an elongated plasma column is created by inner-shell photoionization within the first few femtoseconds of the XFEL pump [19]. The core-excited ions Auger decay within a few femtoseconds and a transient population inversion of femtosecond duration is established. This inversion forms the basis for an x-ray lasing transition. The gain of the XRL depends on the linewidth of the lasing transition. Since the inner-shell photoionization happens on an ultrafast time scale of a few femtoseconds, the ion temperature in the plasma column is expected to remain close to room temperature during the time of amplification. This opens the pathway to very narrow high-gain lasing transitions, with their width being determined only by lifetime broadening of the lower and upper lasing states. The geometry of the x-ray laser is determined by the focus of the XFEL and at a micrometer focal spot size, a gain region several millimeters in length can be achieved [20]. Due to the small aspect ratio, lasing in a single transverse mode is expected. The beam divergence has the same magnitude as the divergence of the focused XFEL beam. Our model calculations demonstrate that saturation of the XRL can be achieved at moderate gas densities.

Amplification of spontaneous emission in the exponential gain region is determined by the small-signal gain. The small-signal gain per atom is defined as

$$g(t) = n_U(t)\sigma_{stim} - n_L(t)\sigma_{abs}. \tag{1}$$

Here n_U and n_L are occupancies of the upper and lower lasing states, and σ_{stim} and σ_{abs} denote the cross section for stimulated emission and absorption,

$$\sigma_{stim} = A_{U\to L}\frac{2\pi c^2}{\omega^2\Delta\omega}, \quad \sigma_{abs} = \sigma_{stim}\frac{g_U}{g_L}, \tag{2}$$

where $A_{U\to L}$ is the Einstein A coefficient for the radiative transition and g_U and g_L are the statistical weights of the

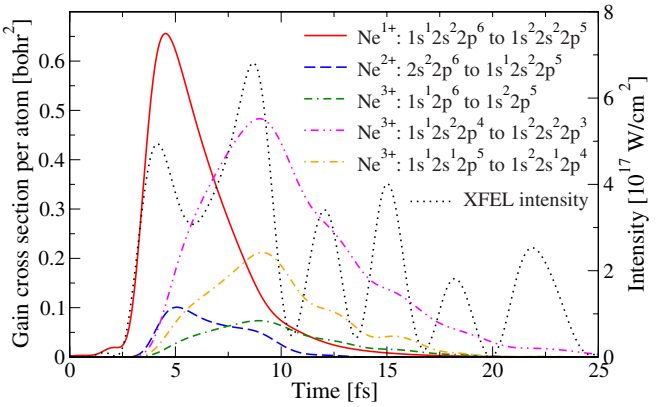

FIG. 1. (Color online) Small-signal gain cross section per atom of singly, doubly, and triply ionized neon for a sample XFEL pulse of 1 keV photon energy. XFEL parameters as described in the text.

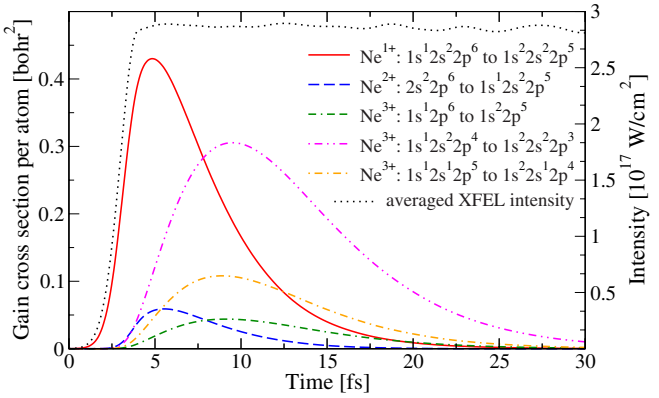

FIG. 2. (Color online) Same as in Fig. 1 but averaged over 10,000 sample pulses.

upper and lower lasing levels. Equation (2) gives the cross sections at the peak of the line, supposing a Lorentzian line shape. The linewidth of the transition $\Delta\omega$ is dominated by the total lifetime of the upper and lower states (Auger lifetime and radiative lifetime) [21]. In the case of the Ne^{1+} $2p^{-1}$-$1s^{-1}$ transition (ω=850 eV), this results in a relative width of $\Delta\omega/\omega=2.9\times10^{-4}$, where we assumed shell-averaged values for Auger and radiative decay rates [22]. The occupancies $n_U(t)$ and $n_L(t)$ are determined by influence of the pumping radiation on an ensemble of single atoms. The occupancies of different configuration states are calculated by solving a system of rate equations, describing valence and core photoionization, Auger, and radiative decay [19]. We treat 63 different channels (configuration states of Neon of charge states up to 10+) and simulate the chaotic intensity profile of the SASE XFEL radiation with a statistical method, following Ref. [23].

Small-signal gain cross sections have been calculated, assuming no influence of the XRL radiation on the level occupancies. Figure 1 shows the small-signal gain cross sections per atom for a sample XFEL pulse of 1 keV photon energy. We assumed 5×10^{12} photons in 100 fs, focused to a 2 μm diameter spot, as expected for LCLS. The highest gains occur in the Ne^{1+} $2p^{-1}$-$1s^{-1}$ and the Ne^{3+} $1s^12s^22p^4$-$1s^22s^22p^3$ lines. The gain maxima are correlated with the intensity peaks of the pump pulse and are separated by a few femtoseconds. The first XFEL spike ionizes an electron from the 1s shell (giving rise to the main lasing line), with a small probability of creating a double hole in the K shell (resulting in the lasing from the Ne^{2+} $2s^22p^6$ state). The width of the Ne^{1+} lasing line is determined by the Auger lifetime of the core hole of 2.75 fs. The dominant Auger decay channel is to Ne^{2+} $1s^22s^22p^4$ which is subsequently core ionized by the second intensity spike of the XFEL pulse, giving rise to the second strongest transition from Ne^{3+} $1s^22s^22p^4$. Due to the chaotic nature of the XFEL pulses, the exact timing and shape of the gain curves vary from pulse to pulse. We therefore averaged the small-signal gain of an ensemble of pulses, shown in Fig. 2. The general trend is similar to the sample shot presented in Fig. 1. The peak gain values of the two strongest lines are on average separated by 5 fs. The temporal width of the lasing lines is 5–10 fs. An exponential growth of the spontaneous radiation can therefore result in intensity spikes of subfemtosecond duration. Due to the nonlinear effects involved [19], the gains resulting from the averaged pump pulse are not equal to the ensemble average of the gain curves. They differ by 10%–30%. The average values and standard deviations of the peak gain and the gain duration are summarized in Table I for different lasing transitions. At atomic densities of 10^{18} cm^{-3} the gain coefficient (in mm^{-1}) is related to the gain cross section (in bohr^2) by $G=2.8g$. Typical peak gain-length products of $G\times L\simeq20$ can therefore be reached with an interaction length of several millimeters, at which the XRL will start to saturate [24].

The saturation intensity is defined as the intensity, at which the rate of stimulated emission equals the exit rate of the upper lasing state and is given by

TABLE I. Saturation intensity, average of the peak value of small-signal gains, and the duration (FWHM) in fs and their standard deviation for an ensemble of 10,000 random pulses for ω_P=1 keV. The pulse parameters correspond to those of Fig. 2.

Ne	Upper state	Gain (a.u.)	STD$_{gain}$	τ (fs)	STD$_\tau$	I_{sat} (W/cm^2)
1+	$1s^12s^22p^6$	0.564	0.102	4.3	1.9	9.3×10^{14}
2+	$2s^22p^6$	0.107	0.061	2.6	1.0	3.4×10^{15}
3+	$1s^12p^6$	0.064	0.017	5.7	2.2	6.3×10^{14}
3+	$1s^12s^22p^4$	0.422	0.105	6.9	2.5	6.6×10^{14}
3+	$1s^12s^12p^5$	0.179	0.058	4.6	1.9	5.6×10^{14}

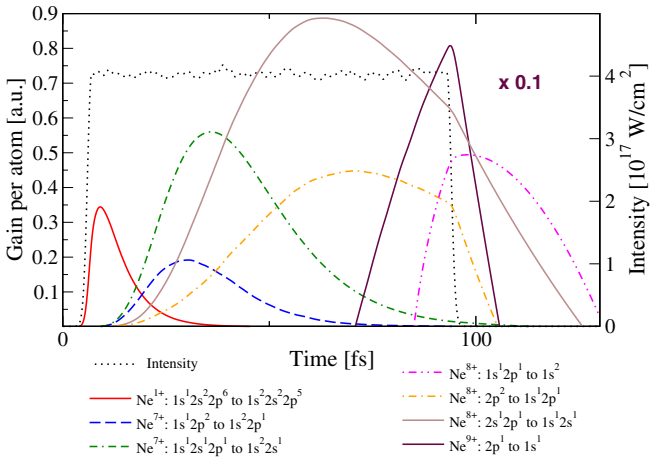

FIG. 3. (Color online) Averaged small-signal gain per atom for ω_P=1.4 keV. Shown are the positive gain coefficients for Ne^1+, Ne^7+Ne^8+, and Ne^9+.

$$I_{sat} = \frac{\Delta\omega_U}{A_{U\to L}} \frac{\omega^3 \Delta\omega}{2\pi c^2}. \tag{3}$$

Since the width of the lasing line $\Delta\omega$ is dominated by the inverse lifetime of the upper state $\Delta\omega_U$, the saturation flux scales as $\Delta\omega_U^2/A_{U\to L}$. This implies that although an enhanced decay rate of the upper states (for lower charge states of neon) decreases the small-signal gain, it increases the saturation intensity. Hence, laser emission from the lower charge states feature shorter pulse duration and higher peak intensity than emission from the highly charged ions. This trend becomes evident by comparing gain cross sections at a higher photon-pump energy, thereby accessing higher charge states. Figure 3 and Table II give results for pumping with 1.4 keV photons. The highest gain occurs in the hydrogenlike Ne^{9+} $2p$-$1s$ transition (ω=1.022 keV). The width of this transition is extremely narrow with $\Delta\omega/\omega \simeq 4\times10^{-6}$ due to the long radiative lifetime of the $2p$ state (~160 fs). To saturate the lasing transition, gas densities on the order of 2×10^{17} cm^{-3} are required. At such densities Stark and collisional broadening are small. The SASE FEL pump has a relative energy width of $\Delta\omega_P/\omega_P \simeq 4\times10^{-4}$, resulting in a longitudinal coherence time $\tau_c \propto \Delta\omega_P^{-1}$ of the order of 2 fs. Exploiting the Ne^{9+} lasing transition, the coherence time of the generated XRL would exceed that of the XFEL pump by an order of magnitude. This would result in XRL pulses of a smooth intensity profile, which would have big advantages in studying nonlinear interactions of x-ray photons with matter [19]. It is important to note that positive gain of the Ne^{9+} $2p$-$1s$ transition can only be achieved by tuning the XFEL photon frequency above the ionization edge of Ne^{9+}, in order to deplete the lower lasing state. Unlike in recently proposed xuv FEL pumped lasing schemes using inner valence electrons [15] where the depletion of the lower lasing level is caused by fast Coster-Kronig transitions, in our scheme the lower lasing levels are depleted by photoionization by the pump. Our scheme is therefore widely applicable and can be extended to any other atomic species by tuning the pump frequency accordingly.

The proposed pumping scheme allows the selection of different lasing transitions by tuning the XFEL energy and changing the gas density accordingly. Tuning below the Ne^{9+} ionization edge, the gain of the Ne^{9+} can be completely suppressed. In this case, gain of Ne^{1+}, Ne^{7+}, and Ne^{8+} lines are of similar magnitude and several lasing lines of different frequency can be saturated. Although the proposed lasing scheme is self-terminating, i.e., each atom can at most contribute a single photon to one lasing line, each atom can successively undergo stimulated emission of independent lasing lines (lines, for which upper and lower states are not directly coupled to states of the other transition). As a consequence, it might be possible to saturate two or more distinct lasing lines, provided that the small-signal gains are of similar strength. The resulting outcome of the x-ray laser would therefore consist of consecutive pulses of distinct color separated by a few femtoseconds.

Given that it seems possible to achieve large gains, we

TABLE II. Same as in Table I but for ω_P=1.4 keV.

Ne	Upper state	Gain (a.u.)	STD$_{gain}$	τ (fs)	STD$_\tau$	I_{sat} (W/cm^2)
1+	$1s^1 2s^2 2p^6$	0.466	0.101	5.3	2.4	9.3×10^{14}
2+	$2s^2 2p^6$	0.051	0.032	2.3	1.1	3.4×10^{15}
3+	$1s^1 2s^2 2p^4$	0.199	0.041	7.2	3.2	6.6×10^{14}
3+	$1s^1 2s^1 2p^5$	0.061	0.023	3.4	1.5	5.6×10^{14}
5+	$1s^1 2p^4$	0.067	0.022	4.0	2.0	2.6×10^{14}
5+	$1s^1 2s^1 2p^3$	0.126	0.040	4.4	2.3	2.0×10^{14}
5+	$1s^1 2s^2 2p^2$	0.092	0.015	10.9	4.9	3.5×10^{14}
7+	$1s^1 2p^2$	0.351	0.090	5.9	4.2	2.6×10^{13}
7+	$1s^1 2s^1 2p^1$	0.506	0.042	26.3	7.6	1.2×10^{13}
8+	$1s^1 2p^1$	0.364	0.198	39.8	28.1	1.1×10^{11}
8+	$2p^2$	0.698	0.234	12.7	12.4	8.3×10^{13}
8+	$2s^1 2p^1$	0.896	0.127	40.6	24.3	3.6×10^{13}
9+	$2p^1$	6.131	2.718	14.9	12.2	4.4×10^{11}

now discuss the expected output properties of an XFEL-pumped XRL. To simulate the output of the lasing transition with highest gain, we apply a one-dimensional model that couples the atomic level kinetics to the laser propagation and amplification. The rate equation for determining the occupation of the upper lasing state $N_U(z,t)$ at position z is

$$\frac{dN_U(z,t)}{dt} = \sum_i \sigma_i^v j(\tilde{t}_z) N_i^S(\tilde{t}_z) + \sum_i \sigma_i^c j(\tilde{t}_z) N_i^S(\tilde{t}_z) - \sigma^{se}[j_+^{\mathrm{XRL}}(z,t) + j_-^{\mathrm{XRL}}(z,t)] N_U(z,t) + \sigma^{abs}[j_+^{\mathrm{XRL}}(z,t) + j_-^{\mathrm{XRL}}(z,t)] N_L(z,t) - [A_{U\to L} + p_U^A + (\sigma_U^v + \sigma_U^c) j(\tilde{t}_z)] N_U(z,t) \quad (4)$$

where σ_i^v and σ_i^c denote the cross section for valence and core photoionization [25], respectively, for a source state with occupation N_i^S and $\tilde{t}_z = t - z/c$. The propagating flux of the pump pulse is denoted by $j(z,t)$ and p_U^A is the total Auger decay rate of the upper lasing state. The second and third rows of Eq. (4) correspond to the stimulated absorption and emission of forward and backward propagating XRL flux j_+^{XRL} and j_-^{XRL}, and the last row describes losses due to spontaneous decay, Auger decay, and photoionization of core and valence shell. The occupation of the lower lasing level is modeled similarly. The XRL flux is determined by

$$\frac{dj_\pm^{\mathrm{XRL}}}{dt} = j_\pm^{\mathrm{XRL}}(z,t) c n_A [\sigma^{se} N_U(z,t) - \sigma^{abs} N_L(z,t)] + \frac{\theta_\pm(z)}{4\pi} A_{U\to L} N_U(z,t) n_A c \mp c \frac{dj_\pm^{\mathrm{XRL}}}{dz}, \quad (5)$$

where $\theta_\pm(z) = 2\pi[1 - (L/2 \mp z)/\sqrt{r^2 + (L/2 \mp z)^2}]$ are the geometrical acceptance angles, allowing propagation in forward and backward directions, n_A is the atomic density, and L is the interaction length and r is the focal radius. Due to the longitudinal pumping, lasing occurs only in forward direction. Results for a typical sample XFEL pulse are presented in Fig. 4, showing the peak intensity and pulse duration [full width at half maximum (FWHM)] of the Ne^{1+} lasing transition as a function of the interaction length for a gas density of 4×10^{18} cm^{-3}. The pulse duration decreases in the exponential gain regime, but as soon as saturation sets in, the pulse duration increases, since the low intensity flanks of the pulses still follow exponential gain, whereas the peak-intensity regions are already saturated. The inset shows the intensity profile of the pump and XRL pulse at the exit. Lasing basically happens during the first intensity maximum of the pump pulse. Our self-consistent gain calculations indicate that peak intensities of 6×10^{16} W/cm^2 can be achieved with subfemtosecond pulse duration.

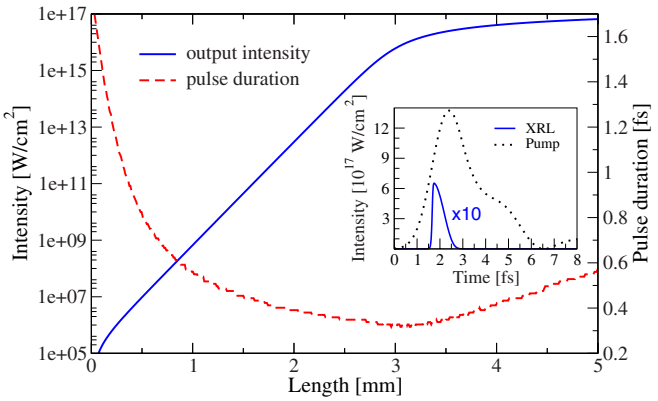

FIG. 4. (Color online) Shown are the output intensity and the pulse duration (FWHM) of the XRL for the Ne^{1+} $1s^{-1}$-$2p^{-1}$ line as function of the interaction length for a gas density of $n=4 \times 10^{18}$ cm^{-3} for an XFEL sample shot. The inset shows the intensity profile of the pump and XRL pulse at the exit of the gain medium.

In this paper we presented a scheme to use XFEL radiation to pump a photoionization inner-shell x-ray laser in an atomic gas. The small-signal gain cross sections for neon show that several XRL lines can be saturated at moderate gas densities and interaction lengths of a few millimeters. Self-consistent gain calculations indicate that subfemtosecond x-ray pulses at peak intensities comparable to the XFEL pump can be achieved. Moreover, the scheme could be exploited to produce a sequence of XRL femtosecond pulses of different wavelengths, temporally separated by a few femtoseconds. This would be a first step for a two-color pump-probe source in the x-ray regime. Adjusting the XFEL pump to higher energies, the scheme can be generalized to heavier atoms and therefore shorter wavelengths.

Work supported by the U.S. Department of Energy under Contract No. DE-AC52-07NA27344; support from the Laboratory Directed Research and Development Program at LLNL is also acknowledged.

[1] D. L. Matthews *et al.*, Phys. Rev. Lett. **54**, 110 (1985).
[2] B. J. MacGowan *et al.*, Phys. Fluids B **4**, 2326 (1992).
[3] Z. Huang and K.-J. Kim, Phys. Rev. ST Accel. Beams **10**, 034801 (2007).
[4] R. Bonifacio, C. Pellegrini, and L. M. Narducci, Opt. Commun. **50**, 373 (1984).
[5] E. L. Saldin, E. A. Schneidmiller, and M. V. Yurkov, Opt. Commun. **148**, 383 (1998).
[6] A. Pietzsch *et al.*, New J. Phys. **10**, 33004 (2008).
[7] A. Cavalleri *et al.*, Nature (London) **442**, 664 (2006).
[8] Z.-H. Loh, M. Khalil, R. E. Correa, R. Santra, C. Buth, and S. R. Leone, Phys. Rev. Lett. **98**, 143601 (2007).
[9] N. Rohringer and R. Santra, Phys. Rev. A **77**, 053404 (2008).
[10] T. Pfeifer, C. Spielmann, and G. Gerber, Rep. Prog. Phys. **69**, 443 (2006).
[11] P. Emma, K. Bane, M. Cornacchia, Z. Huang, H. Schlarb, G. Stupakov, and D. Walz, Phys. Rev. Lett. **92**, 074801 (2004).
[12] Y. Ding, A. Brachmann, F.-J. Decker, D. Dowell, P. Emma, J.

Frisch, S. Gilevich, G. Hays, Ph. Hering, Z. Huang, R. Iverson, H. Loos, A. Miahnahri, H.-D. Nuhn, D. Ratner, J. Turner, J. Welch, W. White, and J. Wu, Phys. Rev. Lett. **102**, 254801 (2009).

[13] N. R. Thompson and B. W. J. McNeil, Phys. Rev. Lett. **100**, 203901 (2008).

[14] Y. Wang *et al.*, Nat. Photonics **2**, 94 (2008).

[15] J. Zhao *et al.*, Opt. Express **16**, 3546 (2008).

[16] K. Lan, E. Fill, and J. Meyer-Ter-Vehn, Laser Part. Beams **22**, 261 (2004).

[17] S. Jacquemot, K. T. Phuoc, A. Rousse, and S. Sebban, *X-ray Lasers 2006* (Springer, New York, 2007).

[18] M. A. Duguay and G. P. Rentzepis, Appl. Phys. Lett. **10**, 350 (1967).

[19] N. Rohringer and R. Santra, Phys. Rev. A **76**, 033416 (2007).

[20] Focusing an XFEL pulse with Gaussian profile to a focal diameter of 2 μm, a focal depth of $\sim$5 mm is achieved. This implies a Fresnel number of 0.2 for a lasing transition at 850 eV and a beam divergence of 0.2 mrad.

[21] Collisional broadening can be ruled out. Assuming a geometric collisional ionization cross section [T. S. Axelrod, Phys. Rev. A **13**, 376 (1976)], the characteristic time scale for electron-ion collisions of typical Auger electrons and photoelectrons will be in the order of 100 fs.

[22] C. P. Bhalla, N. O. Folland, and M. A. Hein, Phys. Rev. A **8**, 649 (1973).

[23] G. Vannucci and M. C. Teich, Appl. Opt. **19**, 548 (1980).

[24] R. C. Elton, *X-ray Lasers* (Academic Press, New York, 1990).

[25] Los Alamos National Laboratory Atomic Physics Codes, http://aphysics2.lanl.gov/cgi-bin/ION/runlanl08a.pl